6548 *Inorg. Chem.* **2009**, *48*, 6548–6554
DOI: 10.1021/ic9004906

Inorganic Chemistry
Article

Redox-Switchable Second-Order Nonlinear Optical Responses of Push−Pull Monotetrathiafulvalene-Metalloporphyrins

Chun-Guang Liu, Wei Guan, Ping Song, Li-Kai Yan, and Zhong-Min Su*

Institute of Functional Material Chemistry, Faculty of Chemistry, Northeast Normal University, Changchun 130024, P. R. China

Received March 12, 2009

The redox-active tetrathiafulvalene (TTF) is a good electron donor, and porphyrin is highly delocalized in cyclic π-conjugated systems. The direct combination of the two interesting building units into the same molecule provides an intriguing molecular system for designing nonlinear optical (NLO) molecular materials. In the present paper, the second-order NLO properties of a series of monoTTF-porphyrins and metalloporphyrins have been calculated by density functional theory (DFT) combined with the finite field (FF) method. Our calculations show that these compounds possess considerably large static first hyperpolarizabilities, $\sim 400 \times 10^{-30}$ esu. Since the TTF unit is able to exist in three different stable redox states (TTF, $TTF^{\bullet+}$, and TTF^{2+}), the redox switching of the NLO response of the zinc^{II} derivative of monoTTF-metalloporphyrin has been studied, and a substantial enhancement in static first hyperpolarizability has been obtained in its oxidized species according to our DFT-FF calculations. The β values of one- and two-electron-oxidized species are 3.6 and 8.7 times as large as that of the neutral compound, especially for two-electron-oxidized species, with a value of 3384×10^{-30} esu. This value is about 3 times that for a push−pull metalloporphyrin, which has an exceptionally large hyperpolarizability among reported organic NLO chromophores. Meanwhile, to give a more intuitive description of band assignments of the electron spectrum and trends in NLO behavior of these compounds, the time-dependent (TD)DFT method has been adopted to calculate the electron spectrum. The TDDFT calculations well-reproduce the soret band and Q-type bands of the monoTTF-porphyrin, and these absorption bands can be assigned to the $\pi \rightarrow \pi^*$ transition of the porphyrin core. On the other hand, the oxidized process significantly affects the geometrical structures of the TTF unit and porphyrin ring, and the two-electron-oxidized species has a planar TTF unit and a high conjugative porphyrin ring. This effect reduces the excited energy, changes the CT feature, and thus enhances its static first hyperpolarizability.

1. Introduction

The large nonlinear optical (NLO) responses in organic molecules arise from highly delocalized π-electron systems. Porphyrins and metalloporphyrins, with large cyclic π-conjugated systems, have been thus investigated as NLO molecular materials.[1] It is well-known that the molecular second-order NLO property depends not only on the nature of the π-conjugated bridge but also on the strength of the donor and acceptor groups. Thus, a large number of electron donor and acceptor groups have been introduced into porphyrins and metalloporphyrins for optimization of the first molecular hyperpolarizability.[2] For example, the zinc^{II} derivative of the push−pull metalloporphyrin (see Chart 1),[2e] bearing the strong donor dimethylaminophenylethynyl and the well-known acceptor nitryl moiety, possesses an exceptionally high resonance-enhanced β (1064 nm), near 5000×10^{-30} esu, obtained with the hyper-Rayleigh light scattering (HRS) technique. It should be noted that it is 10-fold larger than that of the theoretical calculations.

Since tetrathiafulvalene (TTF) is also an efficient electron donor group (Chart 2),[3] a combination of TTF chemistry and

*To whom correspondence should be addressed. E-mail: zmsu@nenu.edu.cn.

(1) de la Torre, G.; Vzquez, P.; Agull-Lpez, F.; Torres, T. *Chem. Rev.* **2004**, *104*, 3723.

(2) (a) Suslick, K. S.; Chen, C. T.; Meredith, G. R.; Cheng, L.-T. *J. Am. Chem. Soc.* **1992**, *114*, 6928. (b) Li, D.; Swanson, B. I.; Robinson, J. M.; Hoffbauer, M. A. *J. Am. Chem. Soc.* **1993**, *115*, 6975. (c) Sen, A.; Ray, P. C.; Das, P. K.; Krishnan, V. *J. Phys. Chem.* **1996**, *100*, 19611. (d) Albert, I. D. L.; Marks, T. J.; Ratner, M. A. *Chem. Mater.* **1998**, *10*, 753. (e) LeCours, S. M.; Guan, H.-W.; DiMagno, S. G.; Wang, C. H.; Therien, M. J. *J. Am. Chem. Soc.* **1996**, *118*, 1497. (f) Priyadarshy, S.; Therien, M. J.; Beratan, D. N. *J. Am. Chem. Soc.* **1996**, *118*, 1504. (g) Yeung, M.; Ng, A. C. H.; Drew, M. G. B.; Vorpagel, E.; Breitung, E. M.; McMahon, R. J.; Ng, D. K. P. *J. Org. Chem.* **1998**, *63*, 7143. (h) Pizzoti; Ugo, R.; Annoni, E.; Quici, S.; Ledoux-Rak, I.; Zerbi, G.; Del Zoppo, M.; Fantucci, P.; Invernizzi, I. *Inorg. Chim. Acta* **2002**, *340*, 70. (i) Ricciardi, G.; Rosa, A.; van Gisbergen, S. J. A.; Baerends, E. J. *J. Phys. Chem. A* **2000**, *104*, 635. (j) Nagatani, H.; Piron, A.; Brevet, P.-F.; Fermin, D. J.; Girault, H. H. *Langmuir* **2002**, *18*, 6647. (k) Zhang, T.-G.; Zhao, Y.; Asselberghs, I.; Persoons, A.; Clays, K.; Therien, M. T. *J. Am. Chem. Soc.* **2005**, *127*, 9710.

(3) (a) González, M.; Martín, N.; Segura, J. L.; Garín, J.; Orduna, J. *Tetrahedron Lett.* **1998**, *39*, 3269. (b) de Lucas, A. I.; Martín, N.; Sánchez, L.; Seoane, C.; Andreu, R.; Garín, J.; Orduna, J.; Slcalá, R.; Willacampa, B. *Tetrahedron* **1998**, *54*, 4655. (c) González, M.; Martín, N.; Segura, J. L.; Garín, J.; Orduna, J. *Tetrahedron* **1998**, *39*, 3269. (d) González, M.; Martín, N.; Segura, J. L.; Seoane, C.; Garín, J.; Orduna, J.; Alcalá, R.; Sánchez, B.; Villacampa, C. *Tetrahedron* **1999**, *40*, 8599. (e) Bryce, M. R. *Adv. Mater.* **1999**, *11*, 11. (f) González, M.; Segura, J. L.; Seoane, C.; Martín, N.; Garín, J.; Orduna, J.; Alcalá, R.; Villacampa, B.; Hernández, V.; Navarrete, T. L. *J. Org. Chem.* **2001**, *66*, 8872.

 Published on Web 06/12/2009

Chart 1. A Zinc^{II} Derivative of a Push−Pull Metalloporphyrin Having Exceptionally High Molecular Hyperpolarizability among the Reported NLO Organic Chromophores

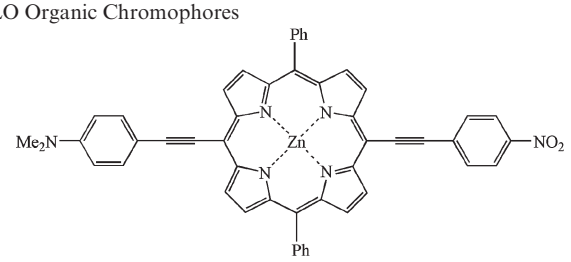

$\beta_{(1064\ nm)} = 4933\times10^{-30}$ esu

Chart 2. Sequential and Reversible Oxidization of TTF Unit

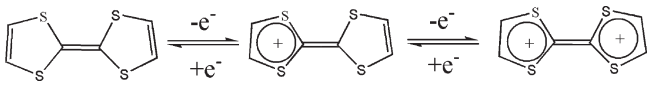

porphyrin chemistry is highly desirable. The direct combination of these two interesting building units into the same molecular system has recently been achieved by the Odense and Angers groups.[4] On the basis of their synthetic scheme, most of the products are tetraTTF-porphyrins, which have a centrosymmetric structure. However, a prerequisite to second-order NLO molecular materials is molecular noncentrosymmetry. A new impetus in this field came to be when the Jeppesen and Sessler groups reported a series of tetra-, bis-, and monoTTF-porphyrins.[5] The electrochemical studies on these TTF-porphyrins showed that the first- and second-oxidation potentials are low (+0.29 V and +0.55 V vs Fc/Fc$^+$ in THF/*n*-Bu_4NPF_6 for monoTTF-porphyrins), and such oxidized species are characteristic of TTF cations.

The redox-active TTF unit has attracted considerable attention because it is able to exist in three different stable redox states (TTF, TTF$^{\cdot+}$, and TTF^{2+}),[6] The TTF unit is a 14-π-electron system. It is nonaromatic according to the Hückel rule because of the lack of π electrons in cyclic conjugation, but its oxidation species, the radical cation TTF$^{\cdot+}$ and dication TTF^{2+}, are aromatic in the Hückel sense. Its oxidation to the radical cation and dication occurs sequentially and reversibly at low potentials ($E_{1/2}{}^1 = 0.34$ V, $E_{1/2}{}^2 = 0.73$ V vs Ag/AgCl in MeCN);[6b] moreover, the TTF radical cation and the TTF dication are thermodynamically stable species. The electron absorption spectra of TTF, TTF$^{\cdot+}$, and TTF^{2+} are decisively different from one another. In terms of the sum-over-states description of the optical nonlinearity, any modification of the absorption spectrum of a molecule contributes to the modification of the hyperpolarizability.[7] Thus, the excellent redox properties of the TTF moiety and good thermodynamic stability of its oxidized species, especially the different aromaticities with respect to the various oxidation states, provide an ideal model for redox switching of NLO responses. The development of materials exhibiting switchable NLO properties can be expected to lead to novel applications for optoelectronic technologies. The ruthenium-based complexes are prototypical examples of redox switching of NLO responses;[8] a series of HRS experiments with ruthenium-based complexes showed that $Ru^{II} \rightarrow Ru^{III}$ oxidation caused the first hyperpolarizability to decrease very substantially.

To elucidate the detailed band assignments of the electron spectrum of monoTTF-porphyrin, the relationship between second-order NLO properties and molecular structure, and redox switching of the NLO responses in detail, we decided to investigate a series of neutral monoTTF-porphyrins and metalloporphyrins, where the strong electron acceptor, the nitryl group, and transition metal ions, Ni^{2+}, Cu^{2+}, and Zn^{2+}, have been introduced for optimization of second-order NLO properties (see Figure 1).

2. Computational Details

The geometries of all compounds were optimized at the B3LYP/6-31 g (d) level.[9] Considering relativistic effects for transition metal ions, the SDD basis set[10] containing the Stuttgart/Dresden effective core potentials was applied for Ni^{2+}, Cu^{2+}, and Zn^{2+} ions. In order to obtain a more intuitive description of the band assignments of the electron spectrum and the trends in the NLO behavior of the studied compounds, time-dependent density functional theory (TDDFT) methods were used to describe the molecular electron spectrum.

The finite field (FF) method was broadly applied because this methodology can be used in concert with the electron structure method to compute hyperpolarizability β.[11] When a molecule is subjected to a static electric field (F), the energy (E) of the molecule is expressed by eq 1:

$$E = E^{(0)} - \mu_i F_i - \frac{1}{2}\alpha_{ij}F_iF_j - \frac{1}{6}\beta_{ijk}F_iF_jF_k - \frac{1}{24}\gamma_{ijkl}F_iF_jF_kF_l - \ldots \quad (1)$$

In this expression, $E^{(0)}$ is the energy of the molecule in the absence of an electronic field, μ_i represents the components of the dipole moment vector, α is the linear polarizability tensor, and β and γ are second-order and third-order polarizability tensors, respectively. The subscripts i, j, and k label x, y, and z components. The molecular Hamiltonian includes a term $(-\boldsymbol{\mu}\cdot\boldsymbol{F})$ describing the interaction between the external uniform static field and the molecule. It is clear that the values of μ, α, β, and γ can be obtained by differentiating E with respect to F. In the present paper, the static first hyperpolarizability β was calculated using the FF method with a field frequency of 0.0010 au at the B3LYP/6-31 g(d) and B3LYP/6-31+g(d) levels (SDD basis set for metal ions). To calculate the dipole moment and the static first hyperpolarizability tensors, the vector from the donor to the acceptor was chosen as the molecular z axis (see Figure 1). The static first hyperpolarizability,

(4) (a) Becher, J.; Brimert, T.; Jeppesen, J. O.; Pedersen, J. Z.; Zubarev, R.; Bjønholm, T.; Reitzel, N.; Jensen, T. R.; Kjaer, K.; Levillain, E. *Angew. Chem., Int. Ed.* **2001**, *40*, 2497. (b) Li, H.; Jeppesen, J. O.; Levillain, E.; Becher, J. *Chem. Commun.* **2003**, 846. (c) Loosli, C.; Jia, C.; Liu, S.-X.; Haas, M.; Dias, M.; Levillain, E.; Neels, A.; Labat, G.; Hauser, A.; Decurtins, S. *J. Org. Chem.* **2005**, *70*, 4988.

(5) Nielsen, K. A.; Levillain, E.; Lynch, V. M.; Sessler, J. L.; Jeppesen, J. O. *Chem.—Eur. J.* **2009**, *15*, 506.

(6) (a) Becher, J.; Jeppesen, J. O.; Nielsen, K. *Synth. Met.* **2003**, *133−134*, 309. (b) Jeppesen, J. O.; Becher, J. *Eur. J. Org. Chem.* **2003**, 3245. (c) Bryce, M. R. *J. Mater. Chem.* **2000**, *10*, 589. (d) Segura, J. L.; Martín, N. *Angew. Chem., Int. Ed.* **2001**, *40*, 1372.

(7) Powell, C. E.; Cifuentes, M. P.; Morrall, J. P.; Stranger, R.; Humphrey, M. G.; Samoc, M.; Luther-Davies, B.; Heath, G. A. *J. Am. Chem. Soc.* **2003**, *126*, 602.

(8) (a) Coe, B. J.; Houbrechts, S.; Asselberghs, I.; Persoons, A. *Angew. Chem., Int. Ed.* **1999**, *38*, 366. (b) Coe, B. J. *Chem.—Eur. J.* **1999**, *5*, 2464. (c) Coe, B. J. *Acc. Chem. Res.* **2006**, *39*, 383.

(9) (a) Becke, A. D. *Phys. Rev.* **1993**, *98*, 5648. (b) Stephens, P. J.; Devlin, F. J.; Chabalowski, C. F; Frishch, M. J. *J. Phys. Chem.* **1994**, *98*, 11623.

(10) Dunning, T. H., Jr.; Hay, P. J. *Modern Theoretical Chemistry*; Schaefer, H. F., III, Ed.; Plenum: New York, 1976; Vol. 3, pp 1−28.

(11) Kanis, D. R.; Ratner, M. A.; Marks, T. J. *Chem. Rev.* **1994**, *94*, 195.

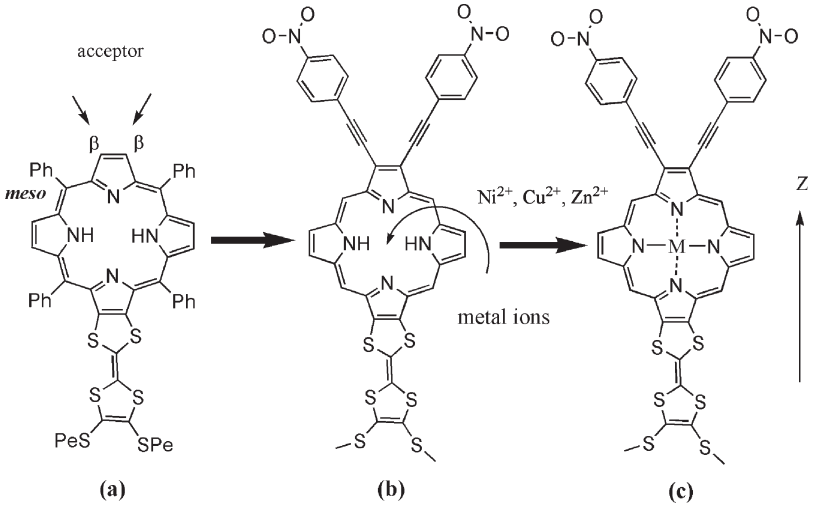

Figure 1. Structural formula of the monoTTF-porphyrin (Pe = n-C_5H_{11}) (a), push−pull monoTTF-porphyrin ligand L (b), and push−pull monoTTF-metalloporphyrins **1**, **2**, and **3** (c).

β_{tot}, for all compounds was calculated by using the following equation (eq 2):

$$\beta_{tot} = (\beta_x^2 + \beta_y^2 + \beta_z^2)^{1/2} \quad (2)$$

where β_i is defined by (eq 3):

$$\beta_i = \beta_{iii} + \sum_{i \neq j} [(\beta_{ijj} + \beta_{jij} + \beta_{jji})/3] \quad (3)$$

All of the calculations in this work were carried out by using the Gaussian 03 program package.[12]

3. Results and Discussion

3.1. Electron Structure of MonoTTF-Porphyrin (L′). The optimized calculations offer a nonplanar structure of monoTTF-porphyrin **L′** (see Figure 2), where the TTF fragment is embowed, the four pyrrole subunits are coplanar, and the dihedral angles between *meso*-phenyl rings and the porphyrin plane are in a range from 81° to 111°. Although the crystal structure is not available, the arrangements of embowed TTF and *meso*-phenyl rings relative to the porphyrin core are rational when compared with the crystal structure of the analogous bisTTF-porphyrin.[5] It should be stressed that the n-C_5H_{11} group on the sulfur atom has been simplified to a methyl group to decrease the computational cost.

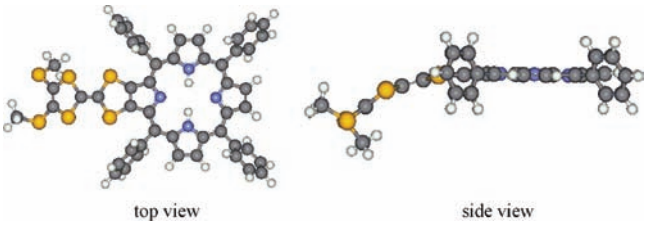

Figure 2. The optimized structure of monoTTF-porphyrin **L′** obtained by B3LYP/6-31 g(d) calculations.

Table 1. TDDFT Results for the Soret and Q-Type Band Arrangement of MonoTTF-Porphyrin **L′** (B3LYP/6-31g(d) calculations in THF)

band type	E(nm)	f_{os}	contributions
soret band	402.2	2.348	HOMO−2 → LUMO (41%)
			HOMO−1 → LUMO + 1 (23%)
Q-band	536.7	0.011	HOMO−1 → LUMO + 1 (57%),
			HOMO−2 → LUMO (42%)
	572.2	0.028	HOMO−1 → LUMO (65%)
			HOMO−2 → LUMO + 1 (40%)

The electron absorption spectrum of monoTTF-porphyrin **L′** in tetrahydrofuran (THF) has been reported.[5] **L′** exhibits a very intense absorption band at 420 nm (soret band) and two Q-type bands with low absorbances at 520 and 610 nm. To rationalize the observed spectral properties, the electron absorption spectrum has been calculated in THF by using the polarized continuum model (PCM) in the Gaussian 03 program package at the B3LYP/6-31 g(d) level. As shown in Table 1, the TDDFT calculation predicts an intense absorption bond at 402 nm that can be assigned to the soret bond, and two weak absorption bands appear at 536 and 572 nm, which are related to the Q-type bands. Thus, TDDFT calculations on the monoTTF-porphyrin offer the key optical transition energy within about 20 nm. Figure 3 shows the electronic level structure based on TDDFT calculations. The intense soret bond corresponds to the HOMO−2 → LUMO and HOMO−1 → LUMO + 1 transitions. The two weak Q-type bands arise from HOMO−1 → LUMO + 1 and HOMO−2 → LUMO transitions (536 nm) and HOMO−1 → LUMO and HOMO−2 → LUMO + 1 transitions (572 nm), respectively. As shown in Figure 3,

(12) Frisch, M. J.; Trucks, G. W.; Schlegel, H. B.; Scuseria, G. E.; Robb, M. A.; Cheeseman, J. R.; Montgomery, J. A., Jr.; Vreven, T.; Kudin, K. N.; Burant, J. C.; Millam, J. M.; Iyengar, S. S.; Tomasi, J.; Barone, V.; Mennucci, B.; Cossi, M.; Scalmani, G.; Rega, N.; Petersson, G. A.; Nakatsuji, H.; Hada, M.; Ehara, M.; Toyota, K.; Fukuda, R.; Hasegawa, J.; Ishida, M.; Nakajima, T.; Honda, Y.; Kitao, O.; Nakai, H.; Klene, M.; Li, X.; Knox, J. E.; Hratchian, H. P.; Cross, J. B.; Bakken, V.; Adamo, C.; Jaramillo, J.; Gomperts, R.; Stratmann, R. E.; Yazyev, O.; Austin, A. J.; Cammi, R.; Pomelli, C.; Ochterski, J. W.; Ayala, P. Y.; Morokuma, K.; Voth, G. A.; Salvador, P.; Dannenberg, J. J.; Zakrzewski, V. G.; Dapprich, S.; Daniels, A. D.; Strain, M. C.; Farkas, O.; Malick, D. K.; Rabuck, A. D.; Raghavachari, K.; Foresman, J. B.; Ortiz, J. V.; Cui, Q.; Baboul, A. G.; Clifford, S.; Cioslowski, J.; Stefanov, B. B.; Liu, G.; Liashenko, A.; Piskorz, P.; Komaromi, I.; Martin, R. L.; Fox, D. J.; Keith, T.; Al-Laham, M. A.; Peng, C. Y.; Nanayakkara, A.; Challacombe, M.; Gill, P. M. W.; Johnson, B.; Chen, W.; Wong, M. W.; Gonzalez, C.; Pople, J. A. *Gaussian 03*, revision C.02; Gaussian, Inc.: Wallingford, CT, 2004.

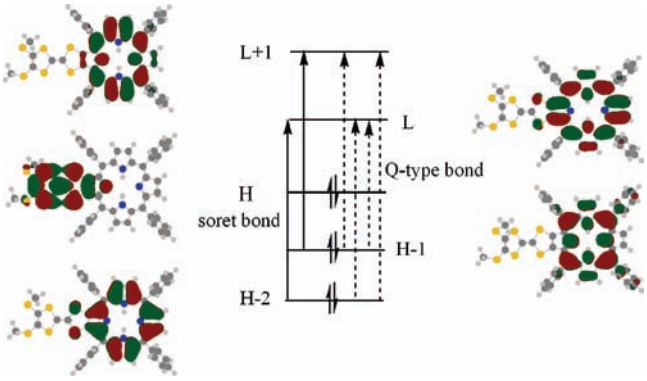

Figure 3. Electron transitions accounting for soret and Q-type bands of monoTTF-porphyrin **L′** calculated by B3LYP/6-31 g(d) in THF.

these molecular orbitals are localized on the porphyrin moiety and display π orbital character, and thus these absorption bands can be assigned to the $\pi \rightarrow \pi^*$ transitions of the porphyrin core.

3.2. Static Second-Order NLO Properties. On the basis of the complex sum-over-states expression, Oudar and Chemla established a simple link between molecular hyperpolarizability and a low-lying energy charge transfer (CT) transition through the two-level model:[13]

$$\beta \propto (\mu_{ee} - \mu_{gg}) \frac{f_{os}}{\Delta E_{ge}^3} \qquad (4)$$

where μ_{gg} and μ_{ee} are the ground and excited state dipole moments, f_{os} is the oscillator strength, and ΔE_{ge} is the transition energy. Those factors ($\mu_{ee} - \mu_{gg}$, ΔE_{ge}, and f_{os}) are all intimately related and are controlled by the electron properties of the donor/acceptor and the nature of the conjugated bridge. The optimal combination of these factors will provide the maximal β value. For example, increasing the conjugated extent of the bridge and the strength of the donor and acceptor groups would enhance the NLO properties. This encourages us to design new functionalized monoTTF-porphyrins by introducing strong electron acceptor and transition metal ions.

The basis set effects are the important issue in ab initio computations for the NLO polarizability.[11] Thus, the static first hyperpolarizabilities of ligand **L′** and complex **3** (see Figure 1) have been calculated at the B3LYP/6-31 g(d) and B3LYP/6-31 + g(d) (SDD basis sets for metal atom) levels. The result indicates that the 6-31 + g(d) basis set provides the larger β value compared to that of the 6-31 g(d) basis set, but the relative values between them do not change largely. The β value of complex **3** is ~18 times as large as that of ligand **L′** according to B3LYP/6-31 + g(d) calculations and ~15 times as large at the B3LYP/6-31 g(d) level (see Table 2). For the large molecules, the large-sized basis sets demand a high computational cost; thus, the static first hyperpolarizabilities of all compounds studied here have been calculated at the B3LYP/6-31 g(d) level.

3.2.1. Push−Pull MonoTTF-Porphyrin. For most of the push−pull porphyrins and metalloporphyrins, the strong donor and acceptor are always attached on the *meso*-phenyl ring,[1] but the dihedral twist of the *meso*-phenyl rings with respect to the porphyrin core always reduces efficient coupling between donor and acceptor moieties and, hence, the effective CT. This leads to a reduction of the first hyperpolarizability.[2d] Thus, we design a new push−pull monoTTF-porphyrin ligand (**L**) with a donor−π conjugated bridge−acceptor (D−π−A) structure; it is different from most of these compounds, where the π-electron spacer groups (alkynyl and phenyl groups) and strong electron acceptor (nitryl group) are attached to the β position of the porphyrin core (see Figure 1). The *meso*-phenyl rings have not been considered because of the large dihedral angle and the relevant position to the TTF electron donor (see Figure 1). The *meso*-phenyl ring has been simplified to a hydrogen atom to decrease the computational cost. The optimized calculations at the B3LYP/6-31 g(d) level show that porphyrin, π-electron spacer groups, and electron acceptor groups are coplanar, while the TTF fragment is still embowed. The dipole moments and static first hyperpolarizabilities of all compounds calculated by DFT have been listed in Table 2. It can be found that introduction of the π-electron spacer groups and strong electron acceptor increases effectively the dipole moment and static first hyperpolarizability of ligand **L**. The β value of ligand **L** increases to 402×10^{-30} esu, 13 times as large as that of monoTTF-porphyrin **L′**.

In order to gain more insight into the second-order NLO response of ligand **L**, we have performed TDDFT calculations on the excited state. The result shows that the first excited state of ligand **L** is generated by the promotion of one electron from the HOMO to the LUMO. As shown in Figure 4, the HOMO localizes on the TTF moiety, and the LUMO delocalizes over the porphyrin unit, phenyl ring, and electron acceptor. This excitation consists of strong CT from TTF to porphyrin, the phenyl

Table 2. Ground-State Dipole Moment (Debye), μ; Static First Hyperpolarizability ($\times 10^{-30}$ esu), β; and Bond-Length Alternation Values, Δr, of Inner and Outer Aromatic Subfragments of Porphyrin Ring (B3LYP/6-31g(d) (SDD basis set on metal ion))

compoud	β_{zzz}	β_{tot}	$\lvert\mu\rvert$	$\Delta r(inner)$	$\Delta r(outer)$
L′	27.7	30.5 (32.4)[a]	2.0		
L	383.9	402.7	9.9	0.028	0.039
1	420.6	431.9	10.3	0.006	0.031
2	426.9	439.7	10.3	0.015	0.032
3	430.1	444.0 (574.7)[a]	10.4	0.027	0.032
$^2\mathbf{3}_{oxidized}{}^+$	1566.7	1591.9	12.6	0.026	0.022
$^3\mathbf{3}_{oxidized}{}^{2+}$	−3695.8	3884.4	15.9	0.006	0.024
$^1\mathbf{3}_{oxidized}{}^{2+}$	−5042.7	5421.8	14.1	0.002	0.023
reference	1193.4	1101.7	9.3		

[a] The static first hyperpolarizabilities of **L′** and **3** also have been calculated at the B3LYP/6-31 + g(d) (SDD basis set on metal ion) level.

Figure 4. The frontier molecular orbitals of ligand L obtained by the B3LYP/6-31 g(d) calculations.

(13) (a) Oudar, J. L.; Chemla, D. S. *J. Chem. Phys.* **1977**, *66*, 2664. (b) Oudar, J. L. *J. Chem. Phys.* **1977**, *67*, 446.

Table 3. TDDFT Results of the MonoTTF-Porphyrin **L** and Metalloporphyrins **1** and **3** for the Low-Energy Excited States with Substantial Oscillator Strength

compound	excited state	E (eV)	f_{os}	contributions
L	S1	1.34	0.001	HOMO → LUMO (95%)
	S5[a]	2.19	0.470	HOMO−2 → LUMO (74%)
1	S1	1.54	0.002	HOMO → LUMO (95%)
	S6[a]	2.18	0.587	HOMO−1 → LUMO (76%), HOMO−2 → LUMO + 1 (14%)
3	S1	1.16	0.0001	HOMO−1 → LUMO (58%) HOMO → LUMO (33%)
	S6[a]	2.14	0.495	HOMO−2 → LUMO (72%) HOMO−3 → LUMO + 1 (21%)
$^1\mathbf{3}_{\mathbf{oxidized}}{}^{2+}$	S1	0.27	0.031	HOMO−1 → LUMO (33%) HOMO → LUMO (18%)
	S14[a]	1.62	0.301	HOMO−14 → LUMO (54%) HOMO−9 → LUMO (24%)

[a] The crucial excited state.

ring, and the electron acceptor. Due to the small overlap between the two orbitals, such electron transition is forbidden, reflecting the small oscillator strength. The crucial excited state, which is the lowest optically allowed excited state with substantial oscillator strength, is also shown in Table 3. According to our TDDFT calculations, these excitations mostly consist of CT from porphyrin to the phenyl ring and electron acceptor. This indicates that the TTF unit does not display electron donor character because the nonplanar embowed structure reduces the molecular conjugation.

3.2.2. Push−Pull MonoTTF-Metalloporphyrins (1, M = Ni; 2, M = Cu; 3, M = Zn). Coordination of a metal ion in a ligand with D−π−A structure can enhance the bridge conjugation and thus increases the first hyperpolarizability.[14] In the present paper, the metal ions Ni^{2+}, Cu^{2+}, and Zn^{2+} have been introduced into ligand **L**. FF calculations indicate that the static first hyperpolarizabilities increase in the order **L** < **1** < **2** < **3**, and zinc^{II} derivative **3** displays the largest first static hyperpolarizability, 444×10^{-30} esu (see Table 2).

The term Δr is defined as the average difference between the bond lengths of two consecutive bonds in the porphyrin. The porphyrin skeleton possesses inner and outer aromatic subfragments, as shown in Figure 5; the bold lines in a and b represent the inner and outer aromatic subfragments, respectively. According to the electron structure calculations and X-ray crystallographic and aromatic ring current studies,[15] the [16] annulene (inner aromatic subfragments) and [18] annulene structures (outer aromatic subfragments) have been proposed as predominant porphyrin conjugative pathways. The bond-length alternation (BLA) values of the inner aromatic subfragments and outer subfragments of all compounds studied here have been listed in Table 2. Although BLA values can not be regarded as the sole parameter in determination of the aromatic character, the small BLA values relative to ligand **L** found in the two conjugative pathways of monoTTF-metalloporphyrins tend to suggest that the metal ions enhance the bridge conjugation. Thus, these metalloporphyrins display a larger static first hyperpolarizability than that of ligand **L**. However, as shown in Table 2, this increase of static first hyperpolarizability of the metalloporphyrin is not sufficient. The β value of the zinc^{II} derivative is only 1.1 times as large as that of ligand **L**. The excited energies of crucial excitation are 2.19, 2.18, and 2.14 eV for compounds **L**, **1**, and **3** according to TDDFT calculations, respectively (see Table 3). It is well-known that the first hyperpolarizability is inversely proportional to the cube of the excited energy and proportional to the oscillator strength; the analogous magnitudes of excited energy and oscillator strength imply a small change of the first hyperpolarizability (see Table 3). The zinc^{II} derivative has the lowest magnitude of excited energy, and thus it gives a small enhancement of the static first hyperpolarizability relative to ligand **L**.

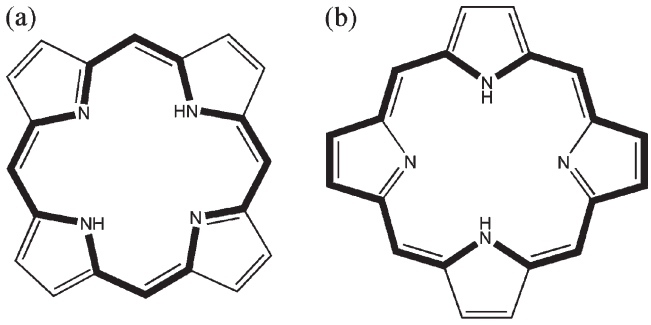

Figure 5. The inner and outer aromatic subfragments of the porphyrin skeleton.

The question we are now concerned with is the orbital transition properties associated with the crucial excited states. We take zinc^{II} derivative **3** as an example to analyze the role of metal ions on the π-conjugated bridge in the CT process. TDDFT calculations show that the crucial excited state is mainly composed of the HOMO−2 → LUMO (72%) and HOMO−3 → LUMO + 1 (21%) transitions. It can be found that the electron densities in HOMO−2 and HOMO−3 are localized on the porphyrin core and metal ion, and the electron densities in LUMO and LUMO + 1 delocalize over the porphyrin core, phenyl ring, and electron acceptor. Obviously, this excitation would give the CT from the porphyrin core and metal ion to the phenyl ring and electron acceptor. This CT nature in metalloporphyrin is similar to that of ligand **L**. The metal ion did not significantly affect the orbital transition, and the TTF unit still does not display the electron donor character in crucial excitation because of the embowed structure in metalloporphyrin according to our TDDFT calculations.

Inspection of the electron density distributions on inner and outer aromatic subfragments in these occupied and unoccupied orbitals showed that the electron density mainly localizes on the outer aromatic subfragment of the porphyrin core (especially in HOMO-2 and LUMO (see Figures 5 and 6)). It should be stressed that all push−pull monoTTF-metalloporphyrins and ligand **L** have analogous electron density distributions. This result indicates that the second-order NLO properties of these

(14) Di Bella, S. *Chem. Soc. Rev.* **2001**, *30*, 355.
(15) (a) Zerner, M. C.; Gouterman, M. *Theor. Chim. Acta* **1966**, *4*, 44. (b) Gouterman, M.; Wagmere, G. *J. Mol. Spectrosc.* **1963**, *11*, 108. (c) Weiss, C.; Kobayashi, H.; Gouterman, M. *J. Mol. Spectrosc.* **1963**, *16*, 415. (d) Kobayashi, H. *J. Chem. Phys.* **1959**, *30*, 1362. (e) Fuhrhop, J.-H. *Angew. Chem., Int. Ed.* **1974**, *13*, 321. (f) Fleischer, E. B. *Acc. Chem. Res.* **1970**, *3*, 105. (g) Hoard, J. L. *Science* **1971**, *174*, 1295. (h) Oth, J. F. M.; Baumann, H.; Gilles, J. M.; Schröder, G. *J. Am. Chem. Soc.* **1972**, *94*, 3498.

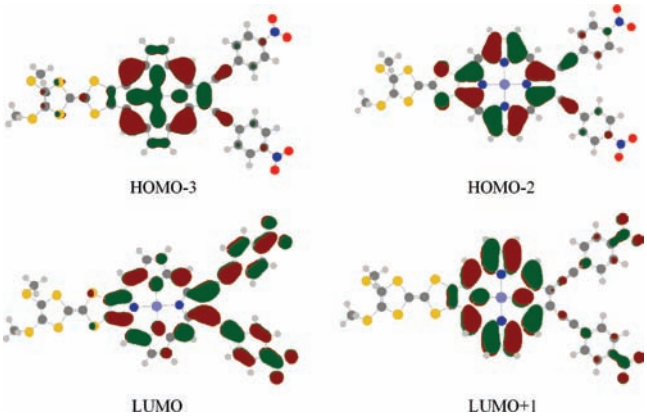

Figure 6. The orbital transitions associated with the crucial excited states of metalloporphyrin **3** obtained by B3LYP/6-31 g(d) (SDD basis set on Zn).

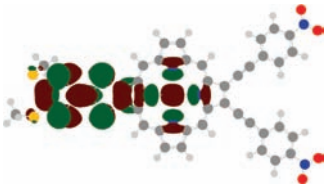

Figure 7. The HOMO of metalloporphyrin **3**.

compounds are related to those of out aromatic subfragment. This supports the idea that the BLA values of out aromatic subfragments for ligand **L** and complexes **1**, **2**, and **3** are almost constant, and thus they have analogous magnitudes of the static first hyperpolarizabilities (see Table 2).

3.3. Redox Switching of NLO Responses. On the basis of the large second-order NLO properties of metalloporphyrin **3**, the static first hyperpolarizability of one- and two-electron-oxidized species of **3** have been calculated. We first analyze the redox properties of this metalloporphyrin.

As shown in Figure 7, the HOMO of **3** mainly localizes on the TTF unit, metal ion, and nitrogen atoms of the pyrrole ring; there is no doubt that the redox properties of the molecule are closely associated with the frontier molecular orbital. It is more likely that the TTF unit, metal ion, and nitrogen atom of the pyrrole ring are the oxidation center of **3**. Unrestricted optimized calculations of one-electron-oxidized species, $^{2}\mathbf{3}_{\mathbf{oxidized}}{}^{+}$ (the one-electron-oxidized species has one unpaired electron and thus a doublet state), were performed to check predictions made by molecular orbital analysis. It can be seen from Figure 8 that the spin density of $^{2}\mathbf{3}_{\mathbf{oxidized}}{}^{+}$ mainly localizes on the TTF unit, metal ion, and nitrogen atom of the pyrrole ring, which is in agreement with the molecular orbital predictions. For two-electron-oxidized species of **3**, two possible spin states (the singlet state $^{1}\mathbf{3}_{\mathbf{oxidized}}{}^{2+}$ and triplet state $^{3}\mathbf{3}_{\mathbf{oxidized}}{}^{2+}$) have been optimized at the UB3LYP/B3LYP/6-31 g(d) level (SDD basis set on metal ion). It can be found that the triplet state $^{3}\mathbf{3}_{\mathbf{oxidized}}{}^{2+}$ is 13.35 kcal/mol more stable than the singlet state $^{1}\mathbf{3}_{\mathbf{oxidized}}{}^{2+}$ in the gas phase and 13.03 kcal/mol more stable than that in THF. The spin density of $^{3}\mathbf{3}_{\mathbf{oxidized}}{}^{2+}$ mainly localizes on the TTF unit, metal ion, and nitrogen atom of the

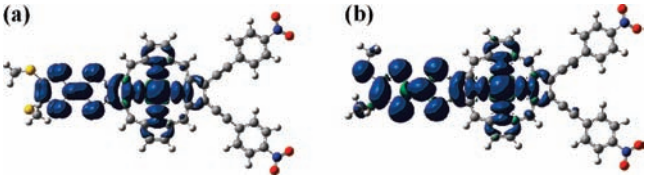

Figure 8. The spin density plots of (a) one- and (b) two-electron-oxidized species of **3** obtained by UB3LYP/6-31 g(d) calculations (SDD basis set on metal ion).

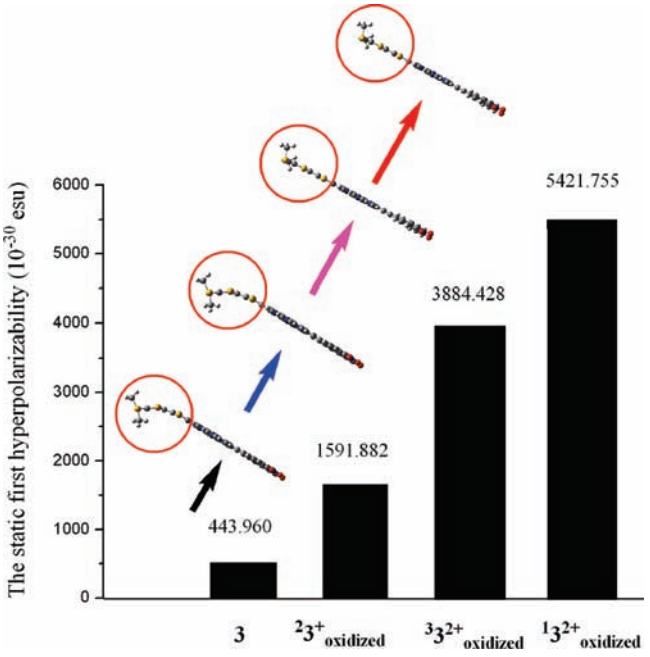

Figure 9. Comparisons of the static first hyperpolarizability of different redox states obtained by B3LYP/6-31 g(d) calculations (SDD basis set on metal ion).

pyrrole ring (see Figure 8), which indicates that the TTF unit, metal ion, and nitrogen atom of the pyrrole ring are still the oxidation center in two-electron-oxidized process.

As mentioned above, the oxidization center of metalloporphyrin **3** is the TTF unit, metal ion, and nitrogen atom of the pyrrole ring. It indicates that the one- and two-electron-oxidized processes will affect the geometrical structure of the TTF unit and porphyrin core. The BLA values of the inner and outer aromatic subfragments of the porphyrin core are listed in Table 2. It can be found that the BLA values of the two conjugative pathways decrease in these oxidized processes, which tends to support the one- and two-electron-oxidized species having better conjugated bridges compared to neutral metalloporphyrin **3**. On the other hand, it is an interesting feature of the TTF unit in these oxidized processes that the embowed TTF unit changes to a planar structure in one- and two-electron-oxidized processes step-by-step (see Figure 9). The two-electron-oxidized species possesses a quite good con-planar structure. All of the results show that the oxidization processes enhance the molecular conjugation and thus increase the static first hyperpolarizability.

According to our FF calculations, the static first hyperpolarizabilities of **3** are strongly sensitive to the

redox state. As shown in Figure 9, the one- and two-electron-oxidized species display large static first hyperpolarizabilities. The β value of the one-electron-oxidized species, $^{2}\mathbf{3}_{\mathbf{oxidized}}{}^{+}$, is ~3.6 times as large as that of **3**; that of the stable two-electron-oxidized species, $^{3}\mathbf{3}_{\mathbf{oxidized}}{}^{2+}$, is ~8.7 times as large as that of **3**; and that of the high-energy two-electron-oxidized species, $^{1}\mathbf{3}_{\mathbf{oxidized}}{}^{2+}$, is ~12.2 times as large as that of **3**. This indicates that the incorporation of electron ejection one-by-one causes a sequential enhancement in the molecular second-order NLO responses. Therefore, the push−pull monoTTF-metalloporphyrins, **3**, could become excellent redox-switchable NLO molecular material. As a reference, we have calculated the static first hyperpolarizability of the zinc^{II} derivative of the push−pull metalloporphyrin (its second-order NLO response is exceptionally high among the reported organic chromophores,[2e] see Chart 1) by using the FF method at the same theoretical level (B3LYP/6-31 g(d) (SDD basis set on metal ion)). This value of 1102×10^{-30} esu is about 3 times as small as that of the stable two-electron-oxidized species $^{3}\mathbf{3}_{\mathbf{oxidized}}{}^{2+}$. Several papers reported that the quantum chemically derived hyperpolarizabilities in the gas phase are always smaller than that in solution, and thus the gas-phase calculations underestimated the second-order NLO responses when compared with the experimental results measured in solution.[11,16] To check the solvent effects on the hyperpolarizability for oxidized species in this work, the static first hyperpolarizability of $^{2}\mathbf{3}_{\mathbf{oxidized}}{}^{+}$ in THF has been calculated by using PCM in the Gaussian 03 program package at the B3LYP/6-31 g(d) level. As expect, the calculated β value of 1962×10^{-30} esu in THF is 1.2 times as large as that in the gas phase.

The electron spectrum of $^{1}\mathbf{3}_{\mathbf{oxidized}}{}^{2+}$ has been calculated at the B3LYP/6-31 g(d) level (SDD basis set on metal ion). It can be found that the first and crucial excited energies of $^{1}\mathbf{3}_{\mathbf{oxidized}}{}^{2+}$ are significantly lower than those of its neutral complex **3**, and the first and crucial excited energies of $^{1}\mathbf{3}_{\mathbf{oxidized}}{}^{2+}$ are ~4.3 and ~1.3 times as small as those of **3**. The relevant low excited energy will generate an increase in the static hyperpolarizability, which is well in agreement with the FF calculations. The crucial excited state of $^{1}\mathbf{3}_{\mathbf{oxidized}}{}^{2+}$ contains the HOMO−14 → LUMO (54%) and HOMO−9 → LUMO (24%) transitions (see Table 3). This leads to a strong CT transition from TTF and methyl sulphide to the metal center and porphyrin ring. It can be found that redox processes significantly affect the electron spectrum, and thus the NLO responses.

(16) (a) Di Bella, S.; Marks, T. J.; Ratner, M. A. *J. Am. Chem. Soc.* **1994**, *116*, 4440. (b) Willetts, A.; Rice, J. E. *J. Chem. Phys.* **1993**, *99*, 426.

4. Conclusion

A systematic DFT calculation was carried out on the monoTTF-porphyrins and metalloporphyrins. The band arrangement of the electron spectrum and second-order NLO properties of these compounds have been analyzed in detail. Our DFT calculations well-reproduce the soret band and Q-type bands of the monoTTF-porphyrin, and these absorption bands can be assigned to the $\pi\rightarrow\pi^*$ transitions of the porphyrin core. The DFT-FF calculations indicate that introduction of the π-electron spacer groups, electron acceptor, and transition metal ions significantly enhances the static first hyperpolarizability of these compounds. The zinc^{II} derivative of the push−pull monoTTF-metalloporphyrin displays the largest β value, 444×10^{-30} esu. On the basis of the excellent redox properties of the TTF unit, which is able to exist in three different stable redox states (TTF, $TTF^{\bullet+}$, and TTF^{2+}), the redox switching of the NLO response of the zinc^{II} derivative of monoTTF-metalloporphyrin has been studied. The results show that the redox processes significantly affect the geometrical structure of the TTF unit and porphyrin, and the one- and two-electron oxidized species have better conjugated bridge and planar structures of the TTF unit relevant to the neutral compound. This effect reduces the excited energy and changes the charge transfer feature and thus enhances the static first hyperpolarizabilities. The β value of one- and two-electron-oxidized species is ~3.6 and ~8.7 times as large as that of its neutral monoTTF-metalloporphyrin. Therefore, the zinc^{II} derivative of the push−pull monoTTF-metalloporphyrins, **3**, could become an excellent redox switchable NLO molecular material.

Acknowledgment. The authors gratefully acknowledge the financial support from the National Natural Science Foundation of China (Project Nos. 20573016 and 20703008), Chang Jiang Scholars Program (2006), Program for Changjiang Scholars and Innovative Research Team in University (IRT0714), the National High-tech Research and Development Program (863 Program 2007AA03Z354), Department of Science and Technology of Jilin Province (20082103), and the Training Fund of NENU's Scientific Innovation Project (NENU-STC07017).